Title

Potein Kinase G Activation Reverses Oxidative Stress and Restores Osteoblast Function and Bone Formation in Male Mice With Type 1 Diabetes

Journal

Diabetes, 67(4)

ISSN

0012-1797

Authors

Kalyanaraman, Hema
Schwaerzer, Gerburg
Ramdani, Ghania
et al.

Publication Date

2018-04-01

DOI

10.2337/db17-0965

Peer reviewed

Protein Kinase G Activation Reverses Oxidative Stress and Restores Osteoblast Function and Bone Formation in Male Mice With Type 1 Diabetes

Hema Kalyanaraman,[1] Gerburg Schwaerzer,[1] Ghania Ramdani,[1] Francine Castillo,[1] Brian T. Scott,[1] Wolfgang Dillmann,[1] Robert L. Sah,[2] Darren E. Casteel,[1] and Renate B. Pilz[1]

Diabetes 2018;67:607–623 | https://doi.org/10.2337/db17-0965

Bone loss and fractures are underrecognized complications of type 1 diabetes and are primarily due to impaired bone formation by osteoblasts. The mechanisms leading to osteoblast dysfunction in diabetes are incompletely understood, but insulin deficiency, poor glycemic control, and hyperglycemia-induced oxidative stress likely contribute. Here we show that insulin promotes osteoblast proliferation and survival via the nitric oxide (NO)/cyclic guanosine monophosphate (cGMP)/protein kinase G (PKG) signal transduction pathway and that PKG stimulation of Akt provides a positive feedback loop. In osteoblasts exposed to high glucose, NO/cGMP/PKG signaling was reduced due in part to the addition of *O*-linked *N*-acetylglucosamine to NO synthase-3, oxidative inhibition of guanylate cyclase activity, and suppression of PKG transcription. Cinaciguat—an NO-independent activator of oxidized guanylate cyclase—increased cGMP synthesis under diabetic conditions and restored proliferation, differentiation, and survival of osteoblasts. Cinaciguat increased trabecular and cortical bone in mice with type 1 diabetes by improving bone formation and osteocyte survival. In bones from diabetic mice and in osteoblasts exposed to high glucose, cinaciguat reduced oxidative stress via PKG-dependent induction of antioxidant genes and downregulation of excess NADPH oxidase-4–dependent H_2O_2 production. These results suggest that cGMP-elevating agents could be used as an adjunct treatment for diabetes-associated osteoporosis.

Bone loss and fractures are frequent and underappreciated complications of type 1 diabetes. Despite improvements in insulin replacement therapy, low bone mineral density and reduced bone mass are observed in most children and adults with type 1 diabetes (1–4). Multiple population-based studies have shown that patients with type 1 diabetes have a two- to fivefold increased risk of fractures, extending across the entire life span; moreover, fractures in patients with diabetes heal slowly, leading to significant morbidity and mortality (3–5). Bone loss in type 1 diabetes is mainly from reduced osteoblast activity; thus, current osteoporosis therapies aimed at inhibiting osteoclasts are inadequate (2,5,6). Patients with type 2 diabetes also have decreased bone formation and increased fracture risk, but bone mineral density may be normal or increased, while bone quality is impaired (1). Mouse models of type 1 diabetes more faithfully recapitulate the human bone disease than models of type 2 diabetes (2,7–9).

Poor glycemic control and diabetes-related vascular complications have emerged as predictors of fractures in most but not all studies of type 1 diabetes (1,3). In a group of patients who had type 1 diabetes for >50 years with excellent glycemic control and a low prevalence of cardiovascular disease, fracture rates were low, suggesting that optimal insulin therapy may protect from both complications (10). Insulin and IGF-1 have important anabolic effects in osteoblasts, as demonstrated in genetic mouse models (11,12). Thus, defective bone remodeling in type 1 diabetes is partly due to insulin deficiency, but the effect of hyperglycemia and hyperglycemia-induced oxidative stress is incompletely defined (13,14).

High glucose concentrations induce oxidative stress by several mechanisms: glucose auto-oxidation, nonenzymatic

[1]Department of Medicine, University of California, San Diego, La Jolla, CA
[2]Department of Bioengineering, University of California, San Diego, La Jolla, CA

Corresponding author: Renate B. Pilz, rpilz@ucsd.edu.

Received 15 August 2017 and accepted 28 December 2017.

This article contains Supplementary Data online at http://diabetes.diabetesjournals.org/lookup/suppl/doi:10.2337/db17-0965/-/DC1.

formation of advanced glycation end products, increased mitochondrial superoxide (O_2^-) production, NAPDH depletion from increased polyol pathway flux, and increased expression or activation of NADPH oxidases (15). Growing evidence indicates increased reactive oxygen species (ROS) and decreased antioxidant defense mechanisms (e.g., thioredoxin) contribute to diabetic tissue damage and bone loss (8,9,16). High glucose also increases flux through the hexosamine pathway, leading to increased uridine diphosphate -*N*-acetyl-glucosamine (UDP-GlcNAc) concentrations, and posttranslational *O*-linked (*O*-)GlcNAc modification of proteins, such as NO synthase (NOS3) and SP1 transcription factors (15,17,18).

O-GlcNAc modification of NOS3 and oxidation of NOS3 cofactors reduce NOS3 activity in endothelial cells of patients with diabetes, causing impaired endothelium-dependent vasodilation, referred to as "endothelial dysfunction" (19). Levels of stable NO metabolites are low in serum and urine of patients with diabetes, suggesting a systemic NO deficiency (20). NO regulates bone formation, as illustrated by osteoblast defects in mice lacking NOS3, and NO donors preserve bone in estrogen-deficient rodents and postmenopausal women (21,22). The major intracellular NO target is soluble guanylate cyclase (sGC), which produces cyclic guanosine monophosphate (cGMP), thereby activating cGMP-dependent protein kinase G (PKG1 and 2). We previously defined proproliferative, antiapoptotic pathways involving cGMP/PKG2-mediated activation of Src, extracellular signal–regulated kinase (ERK)-1/2, Akt, and β-catenin in osteoblasts and osteocytes (23–25). We now show that each step of the NO/cGMP/PKG pathway is impaired in osteoblasts and bones of mice with type 1 diabetes and that restoring cGMP synthesis reduces oxidative stress, recovers osteoblast functions, decreases osteocyte apoptosis, and prevents bone loss in the insulin-deficient mice.

RESEARCH DESIGN AND METHODS

Animal Experiments

All mouse procedures were approved by the University of California, San Diego Institutional Animal Care and Use Committee. Male C57Bl/6 mice (11 weeks old) from Envigo/Harlan were housed at three to four animals per cage in a temperature-controlled environment with a 12-h light/dark cycle and fed the standard Teklad Rodent Diet with ad libitum access to food and water. Male mice were used to avoid the confounding effects of estrogens on NO/cGMP signaling (22,26). After 1 week of acclimatization, mice weighing 19–22 g were randomly divided into three groups. Groups 1 and 2 (12 mice each) received streptozotocin at 40 mg/kg/day intraperitoneally for 5 days, and group 3 (controls, 9 mice) received vehicle injections (7). Glucose was measured in tail vein blood 13 days after the start of the injections. Mice with a blood glucose concentration of >270 mg/mL were considered diabetic. Six streptozotocin-administered mice with blood glucose <270 mg/mL were excluded. Mice in groups 1 and 2 (8 and 10 mice, respectively) received vehicle or cinaciguat at 10 μg/kg/day intraperitoneally 6 days/week from day 21 through day 48. This dose of cinaciguat did not significantly reduce systolic blood pressure (<10 mmHg) and is sufficient to prevent bone loss in ovariectomized mice (26). Double calcein labeling was performed by intraperitoneal injection of calcein (25 mg/kg) at 7 and 4 days before euthanasia. Mice were euthanized 1 h after the last drug or vehicle injection by CO_2 intoxication and exsanguination.

Cell Culture

Primary osteoblasts (POBs) and bone marrow stromal cells (BMSCs) were isolated from long bones (22,24) of control mice (Con), mice administered streptozotocin plus vehicle (DM), and mice administered streptozotocin plus cinaciguat (DM+Cin). Cells were cultured in 10% FBS-containing DMEM with 5 mmol/L glucose (Con), 25 mmol/L glucose (DM), or 25 mmol/L glucose plus 100 nmol/L cinaciguat (DM+Cin). POBs were also isolated from mice carrying floxed *prkg2* alleles ($prkg2^{f/f}$) and were infected with an adenovirus encoding CRE recombinase, as previously described (22). Human POBs were explant cultures from trabecular bone fragments obtained from knee replacement operations for osteoarthritis, according to an institutionally approved protocol (24); none of the patients had diabetes. Cells were grown in DMEM with 10% FBS and 25 mmol/L glucose, unless noted otherwise. All POBs were used at passages 1–5 and characterized after differentiation in medium supplemented with ascorbate (0.3 mmol/L) and β-glycerolphosphate (10 mmol/L), as previously described (24).

Quantitative RT-PCR

Femurs were cleaned of surrounding soft tissue, including the periosteum, ~1 mm was cut off the ends, and the bone marrow was flushed out before samples were snap frozen in liquid nitrogen. RNA was purified from pulverized bone shafts and reverse transcribed; PCR was performed using a MX3005P real-time PCR detection system with Brilliant II SYBR Green Mix (Agilent Technologies) (22). Primer sequences are in Supplementary Tables 3 and 4; all primers were tested with serial cDNA dilutions. Relative changes in mRNA expression were analyzed using the $2^{-\Delta\Delta Ct}$ method, with 18S and *tuba1* serving as internal references. Mean ΔCt values (gene of interest minus reference gene) measured in vehicle-treated control groups were assigned a value of 1 (22).

Amplex Red Assay for H_2O_2

Human POBs were seeded at 4×10^4 cells/well in 96-well plates and incubated in 0.1 mL of reaction mixture containing 50 μmol/L Amplex Red and 0.1 units/mL horseradish peroxidase. Fluorescence was measured every 2 min using 540 nm excitation and 590 nm emission wavelengths.

MitoSOX Red Detection of Mitochondrial O_2^-

Human POBs seeded on glass cover slips were loaded with 1 μmol/L MitoSOX Red for 10 min at 37°C. After washing, fluorescence microscopy was performed on live cells using 515 nm excitation and 580 nm emission wavelengths.

Assay of Lipid Peroxidation Products

POBs (5×10^5 cells/well) were lysed in 0.15 mL ice-cold radioimmunoprecipitation assay buffer and sonicated three times for 5 s. To 0.1 mL of cell lysate or serum, 0.2 mL 10% trichloroacetic acid and 0.3 mL 0.67% thiobarbituric acid was added, and samples were boiled for 45 min. The thiobarbituric acid adducts were extracted in butanol and measured using 515 and 553 nm as excitation and emission wavelengths, respectively. Malondialdehyde standards were from Cayman.

Quantitation of NO_x and cGMP

NO production was measured based on nitrite and nitrate accumulation in the medium, using a two-step colorimetric assay: nitrate was first converted to nitrite by nitrate reductase, and then nitrite was measured spectrophotometrically based on the Griess reaction (22). cGMP concentrations were measured using an ELISA kit (Biomedical Technologies) according to the manufacturer's protocol.

Western Blotting and Immunofluorescence Staining

Western blotting was performed using the antibodies described in Supplementary Table 2. Protein carbamylation was detected using the OxyBlot Protein Oxidation Detection Kit (Millipore EMD). Immunofluorescence staining with antibodies specific for BrdU, cleaved caspase-3, or 8-OH-deoxyguanosine (1:100 dilution) was done as previously described (26). Images were analyzed with a Keyence BZ-X700 fluorescence microscope.

Bone Histomorphometry and Staining of Bone Sections

Tibiae were fixed in 70% ethanol, dehydrated, embedded in methyl-methacrylate, and sectioned at the University of Alabama at Birmingham Center for Metabolic Bone Disease. An investigator blinded to the treatment of the mice identified trabecular osteoblasts and osteoclasts on Masson's trichrome–stained sections and assessed fluorochrome labeling on unstained sections (27). Trabecular and cortical bone were analyzed between 0.25 and 2.25 mm or between 0.25 and 4.25 mm, respectively, distal to the growth plate. TUNEL staining of deplasticized sections was performed as previously described (26). For 8-OH-deoxyguanosine staining, sections were treated with proteinase K (10 mg/mL) for 7 min, followed by treatment with 0.2% Triton X-100 for 15 min. Anti–8-OH-deoxyguanosine antibody (1:50 dilution) was followed by goat anti-mouse horseradish peroxidase antibody (1:200), and incubation with 3,3-diaminobenzidine (Vector Laboratories). Blood vessel density was measured based on staining with anti-CD31 antibody (1:100). Clusters of at least two endothelial cells with anti-CD31 membrane staining, separate from other microvessels, were counted as individual vessels. Slides were scanned with a Hamamatsu NanoZoomer 2.0 HT System and analyzed using Digital Pathology NDP.view2 software (22).

Micro-Computed Tomography

Ethanol-fixed tibiae were scanned using a SkyScan 1076 (Bruker, Kontich, Belgium) micro-CT scanner at a voxel size of 9 μm, applying an electrical potential of 50 kV and current of 200 μA, and using a 0.5-mm aluminum filter. A beam-hardening correction algorithm was applied before image reconstruction with DataViewer and CTAn software (Bruker). Cortical bone was analyzed by automatic contouring 3.6–4.5 mm distal to the proximal growth plate, using a global threshold to identify cortical bone and eroding 1 pixel to eliminate partial volume effects. Trabecular bone was analyzed by automatic contouring of the proximal tibial metaphysis 0.36–2.1 mm distal to the growth plate. An adaptive threshold (using the mean maximum and minimum pixel intensity values of the surrounding 10 pixels) was used to identify trabecular bone (28).

Statistical Analyses

Graph Pad Prism 5 software was used for two-tailed Student *t* test to compare two groups or one-way ANOVA with Bonferroni posttest analysis to compare more than 2 groups. $P < 0.05$ was considered significant.

RESULTS

Insulin Enhances Osteoblast Proliferation and Survival via NO/cGMP/PKG2

Insulin treatment of human or murine POBs activated Akt, induced NOS3 Ser^{1177} phosphorylation (a stimulatory site targeted by Akt), and enhanced NO production; these effects were prevented when Akt activation was blocked by LY294002 or MK2206 (Fig. 1*A* and *B* and Supplementary Fig. 1*A*; the NOS inhibitor L-NAME served as a control). These results suggest insulin increases NO synthesis in osteoblasts via Akt phosphorylation of NOS3, similar to the effects of insulin's in endothelial cells (29). Insulin-induced Akt and ERK activation in POBs was reduced by >50% when NOS, sGC, or PKG were inhibited pharmacologically or when PKG2 expression was knocked out by CRE-mediated recombination (Fig. 1*C*–*G*). Correspondingly, insulin stimulation of osteoblast proliferation and survival was largely PKG2-dependent (Fig. 1*H* and *I* and Supplementary Fig. 1*B*).

Together with our previous data showing NO/cGMP regulation of osteoblast proliferation and survival via ERK and Akt (24,25), these results indicate that the anabolic effects of insulin on osteoblasts require NO/cGMP/PKG2 signaling and point toward a positive feedback loop, where insulin-induced NOS3 stimulation is enhanced by PKG2 activation of Akt (Fig. 1*J*). Proproliferative and antiapoptotic insulin signals are reduced when this feedback loop is interrupted by NOS, sGC, or PKG inhibition, or *prkg2* gene knockout.

NOS Activity Is Reduced in POBs From Diabetic Mice and Human POBs Exposed to High Glucose

We isolated POBs from mice with streptozotocin-induced diabetes and control mice, and cultured them in medium containing "high" (25 mmol/L) or physiological "low" (5 mmol/L) glucose concentrations, respectively, to mimic in vivo conditions. Basal NO production was reduced by ~50% in osteoblasts from diabetic compared with control

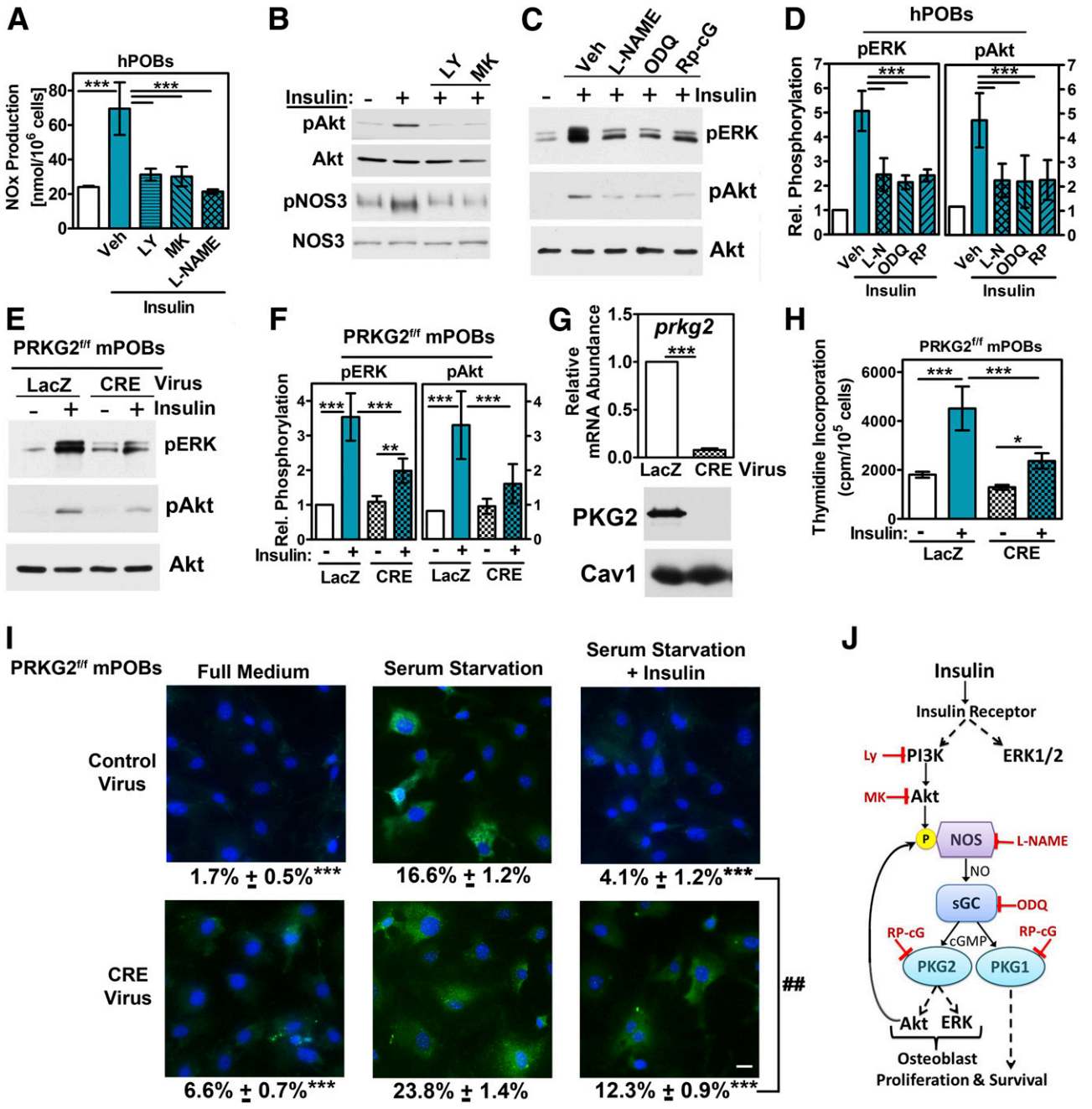

Figure 1—Insulin signaling via NO/cGMP/PKG2 in POBs. *A–D*: Human (h)POBs were treated with pharmacological inhibitors of PI3K (LY294002, 10 μmol/L), Akt (MK2206, 10 μmol/L), NOS (L-NAME, 4 mmol/L), sGC (ODQ, 10 μmol/L), PKG (Rp-CPT-PET-cGMPS, 50 μmol/L), or vehicle (Veh) for 1 h before stimulation with insulin for 20 min. ODQ, 1H-(1,2,4)oxadiazolo(4,3-*a*)quinoxalin-1-one. *A*: Stable NO_x metabolites (nitrite +nitrate) were measured in the medium by Griess reaction. Phosphorylation (p) of Akt (Ser^{473}), NOS3 (Ser^{1177}), and ERK-1/2 (Thr^{202}/Tyr^{204}) was assessed with phospho-specific antibodies (*B* and *C*) and densitometry scanning of Western blots (*D*). *E–G*: Murine (m)POBs containing "floxed" *prkg2*$^{f/f}$ alleles were infected with control virus (LacZ) or virus expressing CRE-recombinase (CRE). *E* and *F*: After 48 h, cells were stimulated with insulin for 10 min to assess ERK and Akt activation. *G*: *prkg2* mRNA (normalized to 18S rRNA) was measured by quantitative RT-PCR, and PKG2 protein (in POB membranes) by Western blotting. *H* and *I*: *prkg2*$^{f/f}$ POBs infected with LacZ or CRE virus were transferred to low serum–containing medium with some cells receiving insulin. *H*: Proliferation was measured by ^{3}H-thymidine incorporation into DNA. *I*: The effect of insulin on apoptosis was assessed by determining the percentage of cells staining for cleaved caspase-3 in the absence of serum (green, DNA counterstained blue with Hoechst 33342). Scale bar = 15 μm. Data represent mean ± SD of three to five independent experiments. $^*P < 0.05$, $^{**}P < 0.01$, and $^{***}P < 0.001$ for the indicated comparisons; in panel *I* $^{***}P < 0.001$ for comparison with serum starvation without insulin and $^{\#\#}P < 0.01$ for the indicated comparison (by ANOVA, except *t* test in *G*). *J*: Insulin activates Akt and ERK downstream of the insulin receptor, and Akt phosphorylation of NOS3 activates the NO/cGMP/PKG2 pathway in osteoblasts to regulate proliferation and survival. Akt phosphorylation of NOS3 also occurs in a positive feedback loop. When NO/cGMP/PKG2 signaling is inhibited, this feedback loop is interrupted, and insulin signaling via ERK and Akt is reduced.

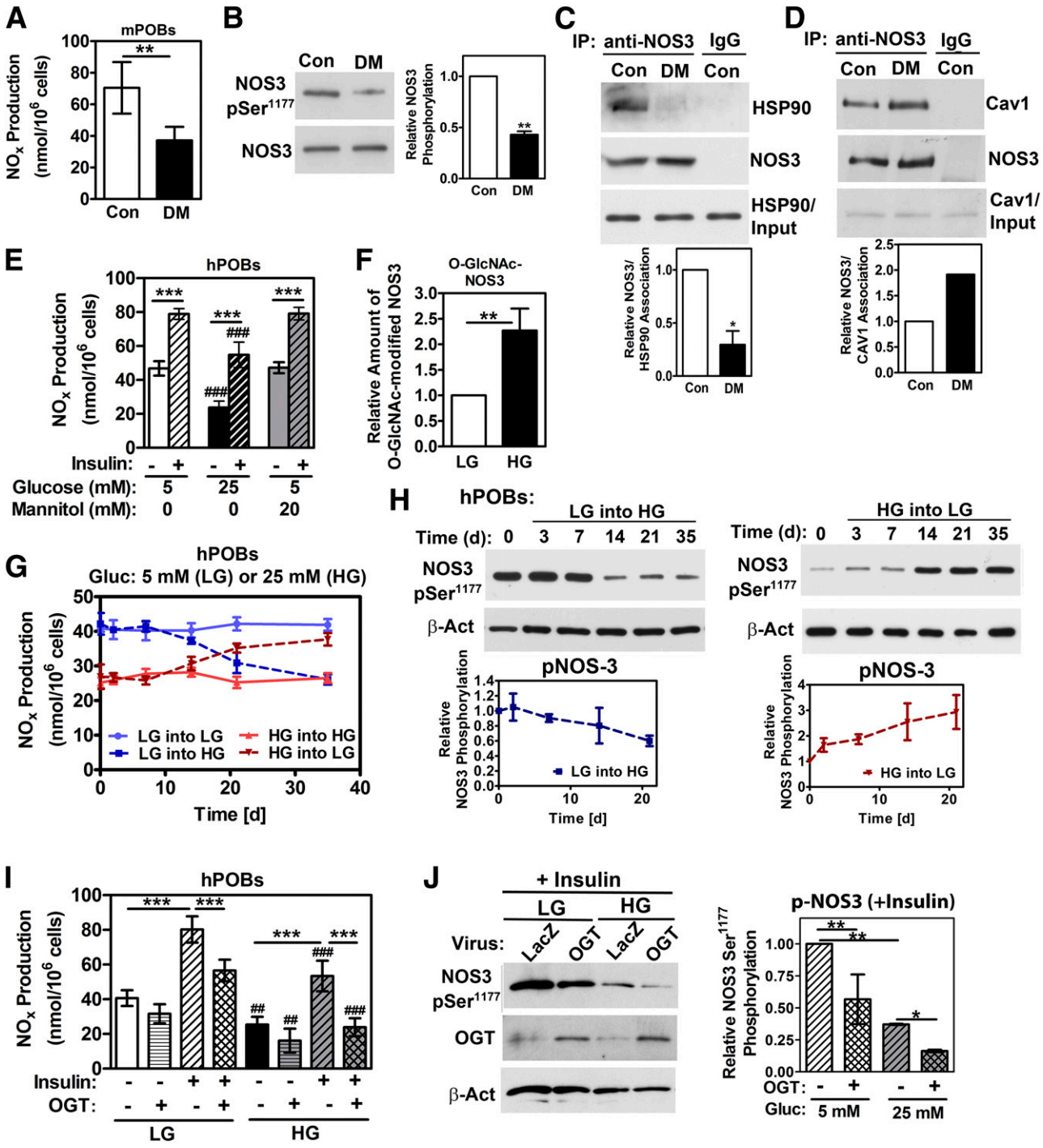

Figure 2—Reduced NOS activity in POBs exposed to high glucose. *A*: Mouse (m)POBs isolated from control (Con) and diabetic mice (DM) were cultured in 5 mmol/L or 25 mmol/L glucose, respectively, and NO_x was measured 2 h after transfer to fresh medium, as in Fig. 1*A*. NOS3 (Ser^{1177}) phosphorylation (p) was analyzed with a phospho-specific antibody (*B*), and NOS3 association with HSP-90 (*C*) or caveolin-1 (*D*) was determined by coimmunoprecipitation (IP) (10% input lysates are shown below). *E*: Human (h)POBs from individuals without diabetes were cultured for 3 weeks in medium with 5 mmol/L (low) glucose (LG) or 25 mmol/L (high) glucose (HG), with some cells in LG receiving 20 mmol/L mannitol; NO_x was measured 2 h after insulin stimulation. *F*: NOS3 was isolated from human POBs cultured in LG or HG by ADP-agarose pull-down, and *O*-GlcNAc modification of the protein was determined on Western blots using the anti–*O*-GlcNAc antibody RL-2. The graph summarizes densitometry scans from three independent experiments. *G* and *H*: Human POBs were maintained in LG or HG medium or were switched from LG to HG and vice versa. NO production (*G*) and NOS3 (Ser^{1177}) phosphorylation (*H*) were measured at 0 and 72 h and then weekly; for each time point, cells were plated at a density of 2×10^4 cells/cm^2. *I* and *J*: Human POBs cultured for 3 weeks in LG or HG were infected with control virus or virus encoding OGT. *I*: Cells received vehicle or insulin for 20 min, and NO_x was measured as in Fig. 1*A*. *J*: NOS3 phosphorylation and OGT expression were assessed in insulin-treated cells. Data represent mean ± SD of three independent experiments (except $n = 2$ in *D*). $^*P < 0.05$, $^{**}P < 0.01$, $^{***}P < 0.001$ for the indicated comparisons, and $\#\#P < 0.01$ and $\#\#\#P < 0.001$ for comparison between the same treatment in HG vs. LG (*A–C*, by *t* test; *E–I*, by ANOVA).

animals, as was NOS3 Ser^{1177} phosphorylation and NOS3 association with HSP90, a positive enzyme regulator (Fig. 2*A–C*) (30). In contrast, NOS3 association with its negative regulator caveolin-1 (30) was increased in diabetic osteoblasts (Fig. 2*D*).

To concentrate on hyperglycemic effects on NO synthesis and simulate diabetic conditions in human POBs, cells from donors without diabetes were cultured for 3 weeks in medium containing high or low glucose. Basal and insulin-stimulated NO production were both reduced in POBs exposed to high glucose compared with cells cultured in low glucose. The differences were not from increased osmolarity, because adding 20 mmol/L mannitol to the 5 mmol/L glucose medium neither affected NO production nor insulin-induced Akt or ERK activation (Fig. 2*E* and Supplementary Fig. 2*A–C*). To determine whether reduced NO production in human POBs cultured in high versus low glucose may be partly related to *O*-GlcNAc modification of NOS3, we isolated the enzyme via ADP-agarose pull-down and probed Western blots with the anti-*O*-GlcNAc antibody RL-2. We found a 2.3-fold increase in NOS3 *O*-GlcNacetylation in cells cultured in high versus low glucose (Fig. 2*F* and Supplementary Fig. 2*D*). These data are in keeping with findings in endothelial cells exposed to high glucose and in vascular tissue from diabetic rats, where *O*-GlcNAc modification of NOS3 on Ser^{1177} reduces NOS activity by interfering with Akt phosphorylation of Ser^{1177} (17,31).

When human POBs were transferred from low to high glucose, NO production and NOS3 Ser^{1177} phosphorylation decreased gradually over ~3 weeks. NO production and NOS3 phosphorylation both recovered with similar kinetics when cells were transferred from high to low glucose (Fig. 2*G* and *H*). Similar results were obtained in POBs isolated from mice with type 1 diabetes (Supplementary Fig. 2*E*). Thus, decreased basal NO synthesis in diabetic POBs is reversible when hyperglycemia is corrected.

To test the effect of *O*-GlcNAc modification on osteoblast NOS activity, we infected human POBs with a viral vector encoding *O*-GlcNAc transferase (OGT), which adds a single GlcNAc in *O*-glycosidic linkage to Ser and Thr residues. OGT expression inhibited insulin-induced NO production and NOS3 Ser^{1177} phosphorylation in low and high glucose medium, and there was a trend toward OGT reducing basal NO synthesis (Fig. 2*I* and *J*). In murine POBs in high glucose, OGT expression decreased basal NO production significantly, whereas expression of *N*-acetylglucosaminidase (GCA), which removes *O*-GlcNAc, increased NO production (Supplementary Fig. 2*F* and *G*). These results are consistent with *O*-GlcNAc modification of NOS3 on Ser^{1177} interfering with NOS3 phosphorylation on this site, thereby reducing NOS activity (17).

Guanylate Cyclase Is Oxidized and NO-Induced cGMP Synthesis Is Impaired in POBs Exposed to High Glucose

The NO donor PAPA-NONOate [(Z)-1-[N-(3-aminopropyl)-N-(n-propyl)amino]diazen-1-ium-1,2-diolate] elicited a dose-dependent increase in the intracellular cGMP concentration in osteoblasts from normal mice in low glucose, but in cells from diabetic mice in high glucose, only the highest PAPA-NONOate concentration elicited a small increase in cGMP (Fig. 3*A*). sGC protein concentrations were similar in both conditions (Fig. 3*B*). To determine whether the decreased NO responsiveness of sGC was due to oxidation of the heme-bound Fe^{2+}, we compared cinaciguat –a NO- and heme-independent sGC activator that can activate oxidized (Fe^{3+}) or heme-free sGC in addition to the reduced (Fe^{2+})-heme-bound enzyme to riociguat, which stimulates only the (Fe^{2+})-heme–containing enzyme (32,33). Cinaciguat increased the intracellular cGMP concentration similarly in osteoblasts from control and diabetic mice, whereas comparable concentrations of riociguat had minimal effect in cells from diabetic mice (Fig. 3*C*). Similarly, PAPA-NONOate and riociguat induced ERK and Akt activation much less effectively in cells from diabetic mice compared with control cells, whereas cinaciguat was equally effective under both conditions (Fig. 3*D* and *E*). The cell permeable ROS scavenger tempol partly restored sGC responsiveness to PAPA-NONOate and riociguat in cells from diabetic mice, providing further support that the sGC heme group is oxidized under diabetic conditions (Fig. 3*F*). Thus, cinaciguat, the prototype of a new class of NO-independent sGC activators under clinical development (32), effectively raises osteoblast cGMP under hyperglycemic conditions.

Expression of *prkg1* and *prkg2* Is Downregulated in POBs Exposed to High Glucose

The main cGMP targets in osteoblasts are cytosolic PKG1 and membrane-bound PKG2, encoded by *prkg1* and *prkg2*, respectively (24). Both enzymes have some overlapping but also distinct functions in promoting osteoblast proliferation, differentiation, and survival (24,25). We found decreased PKG1 and 2 protein and *prkg1* and *2* mRNA in osteoblasts from diabetic mice compared with control mice, whereas *nos3* and *gucy1* mRNAs (encoding NOS3 and the common sGC-β1 subunit) were unchanged (Fig. 3*G–I*). Switching human osteoblasts from low to high glucose medium decreased *prkg1* and *2* mRNAs over 2–3 weeks, and changing cells from high to low glucose increased both mRNAs over a similar time course (Fig. 3*J*). The stability of both mRNAs was not altered in high versus low glucose medium (Supplementary Fig. 3*A* and *B*).

To determine whether glucose-induced oxidative stress contributed to transcriptional downregulation of *prkg1* and *2*, we treated osteoblasts in high glucose medium with tempol. Tempol increased *prkg1* and *2* mRNAs in human and murine POBs in high glucose to concentrations found in low glucose–containing medium; concomitantly, the drug decreased the intracellular concentration of malondialdehyde, a lipid oxidation marker (Fig. 3*K* and Supplementary Fig. 3*C* and *D*).

We have shown that high glucose–induced *O*-GlcNAc modification of the transcription factor SP1 leads to

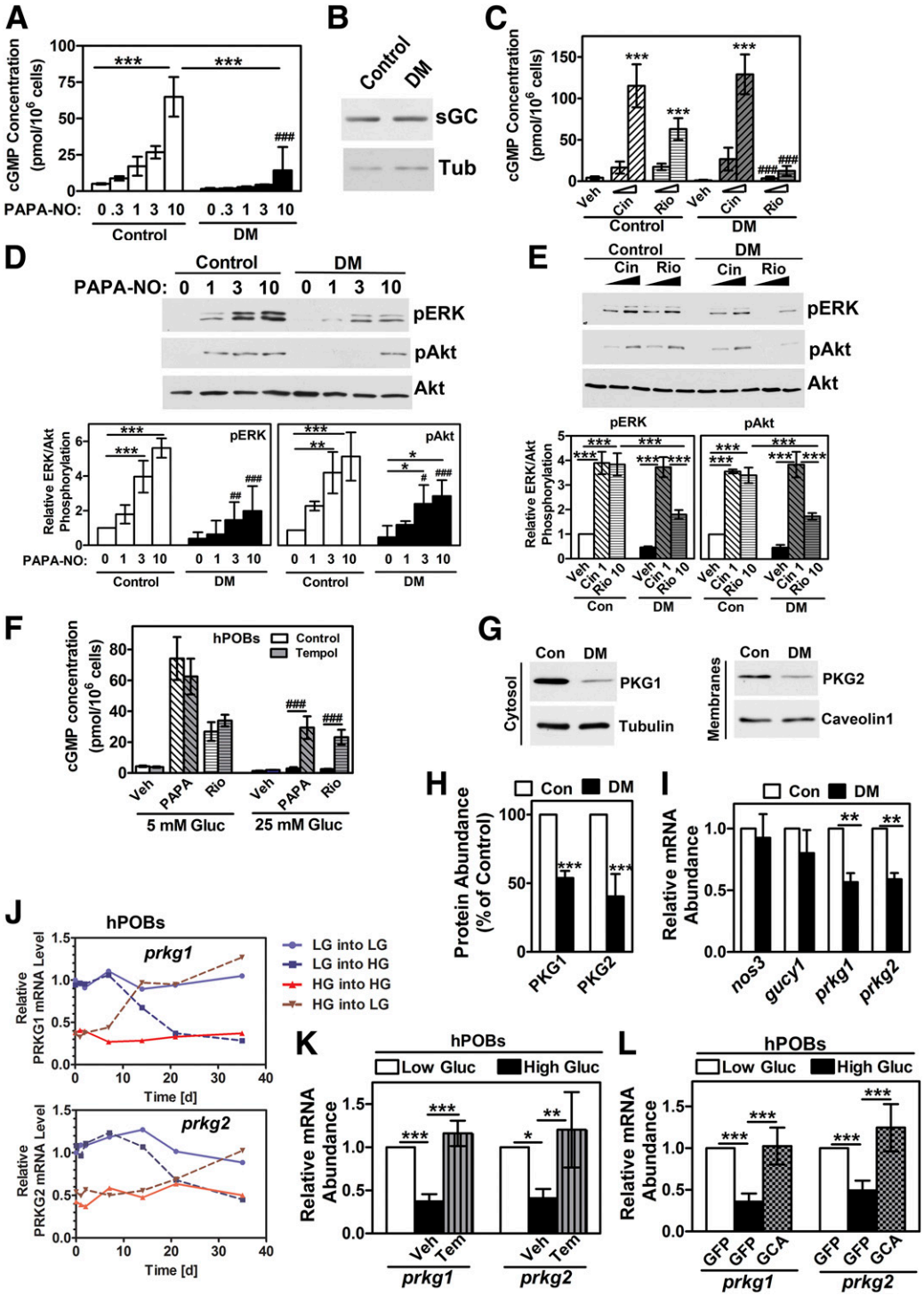

Figure 3—Oxidized guanylate cyclase and reduced *prkg1* and *prkg2* expression in POBs exposed to high glucose. *A–E* and *G–I*: POBs were isolated from control (Con) or diabetic mice (DM) and cultured as in Fig. 2*A*. *A*: Cells were stimulated with the NO donor PAPA-NONOate (0.3–10 μmol/L) for 30 min, and cGMP was measured by ELISA. *B*: Expression of sGC was assessed by Western blotting using an antibody for the common β1 subunit, with α-tubulin (Tub) as the loading control. *C*: Cells were stimulated with vehicle (Veh), cinaciguat (Cin, 0.1 and 1 μmol/L) or riociguat (Rio, 1 and 10 μmol/L) for 30 min, and cGMP was measured by ELISA. *D* and *E*: Cells were treated with PAPA-NONOate, Cin, or Rio for 10 min; ERK and Akt phosphorylation (p) were assessed as in Fig. 1*C*. *F*: Human (h)POBs cultured in 5 or 25 mmol/L glucose for 3 weeks were treated with 200 μmol/L tempol for 48 h before stimulation with 3 μmol/L PAPA-NONOate or 10 μmol/L Rio for 30 min; cGMP was measured as in panel *A*. *G*: Cytosolic and membrane fractions from control and diabetic POBs were analyzed by Western blotting with antibodies for PKG1, tubulin, PKG2, and caveolin-1. *H*: Blots were quantified by densitometry. *I*: *nos3*, *gucy1* (sGC common β1 subunit), and *prkg1* and *2* mRNAs were quantified by RT-PCR and normalized to 18S rRNA in control and diabetic POBs; expression in control POBs was assigned a value of 1. *J*: After 3 weeks in medium with 5 mmol/L (low) glucose (LG) or 25 mmol/L (high) glucose (HG), human POBs were maintained in the same medium or were switched from LG to HG and vice versa, and *prkg1* and *2* mRNAs were measured as in panel *I*. *K* and *L*: Human POBs cultured in LG or HG for 3 weeks received vehicle vs. tempol (Tem, 200 μmol/L) or were infected with control virus encoding green fluorescent protein (GFP)

decreased promoter activity and expression of target genes and that SP1 positively regulates *prkg1* expression (18). Expressing GCA in POBs in high glucose medium restored *prkg1* and *2* mRNAs to concentrations found in low glucose (Fig. 3*I*). Thus, decreased *prkg1* and *2* transcription under diabetic conditions is likely caused by oxidative stress and *O*-GlcNAc modification of transcriptional regulators.

Cinaciguat Restores Proliferation and Differentiation of Preosteoblasts Exposed to High Glucose

POBs isolated from diabetic mice and cultured in high glucose showed lower BrdU incorporation into DNA, and, when differentiated in vitro, produced less alkaline phosphatase (ALP) and mineralized less well than POBs isolated from control mice cultured in low glucose (Fig. 4*A–D*; POBs in Fig. 4*C* and *D* were postconfluent when they were switched to differentiation medium). Treating diabetic mice with cinaciguat (see Fig. 7*A*, below) and culturing POBs from these mice in high glucose in the presence of 100 nmol/L cinaciguat returned BrdU incorporation, ALP production, and cell mineralization to values found in cells from control mice in low glucose (Fig. 4*A–D*). In addition, cinaciguat restored mRNA expression of osteoblast marker genes and *c-fos* in osteoblasts from diabetic mice to that of control mice (Fig. 4*E* and *F*). BMSCs isolated from diabetic mice and cultured in high glucose generated fewer ALP-producing colonies and expressed lower amounts of osteoblast-specific genes compared with cells from control mice, and once again, cinaciguat restored these functions (Fig. 4*G–I* and Supplementary Fig. 4).

Cinaciguat Reduces Oxidative Stress in POBs Exposed to High Glucose

We assessed oxidative stress by measuring whole-cell H_2O_2 production, lipid, protein, and DNA oxidation, activation of the stress kinases c-Jun N-terminal kinase (JNK) and p38, and mitochondrial O_2^- production (15). In POBs isolated from diabetic mice and in human POBs cultured in high glucose, H_2O_2 production was higher than in control POBs in low glucose, and cinaciguat reduced H_2O_2 production significantly (Fig. 5*A* and *B*). The cGMP analog 8-*p*-chlorophenylthio–cGMP (8-CPT–cGMP) and the antioxidant tempol decreased H_2O_2 production comparable to cinaciguat (Fig. 5*B*). The effect of cinaciguat was mediated by PKG2, because the drug was ineffective in *prkg2*-deficient osteoblasts (Fig. 5*C*). Protein, lipid, and DNA oxidation and p38 and JNK phosphorylation were increased in cells exposed to high glucose, and cinaciguat largely reversed these changes (Fig. 5*D–J* and Supplementary Fig. 5*A–C*). Again, 8-CPT–cGMP and tempol had similar effects as cinaciguat, and the effects of cinaciguat on lipid peroxidation were absent in *prkg2*-deficient osteoblasts (Fig. 5*E* and *F*).

In contrast to findings in endothelial cells (19), we found no evidence that NOS uncoupling contributed to H_2O_2 production in osteoblasts in high glucose (Supplementary Fig. 5*D*). Using the mitochondrial O_2^- indicator MitoSOX Red, we found increased mitochondrial O_2^- production in human POBs exposed to high glucose compared with POBs cultured in low glucose. Cinaciguat reduced mitochondrial O_2^- production toward values seen in low glucose (Supplementary Fig. 5*E*; antimycin A was used as a positive control). Thus, cinaciguat reduces oxidative stress in osteoblasts under high glucose conditions.

Cinaciguat Regulates Thioredoxin-Related Genes and NADPH Oxidase 4, Which Is a Major Source of ROS in POBs Exposed to High Glucose

Because transgenic expression of thioredoxin (*txn1*) reduces oxidative stress and partly prevents diabetes-induced bone loss in mice with type 1 diabetes (16), we determined the effect of hyperglycemia and cinaciguat on *txn1* and thioredoxin-related genes. Compared with normoglycemic conditions, we found reduced expression of the antioxidant genes *txn1*, *txnrd1* (thioredoxin reductase), and *prdx1* (thioredoxin peroxidase) in osteoblasts under hyperglycemic conditions, with almost full recovery after cinaciguat treatment (Fig. 6*A*). The pro-oxidant gene *txnip* (thioredoxin-interacting protein) was regulated in the opposite direction (Fig. 6*A*). Thioredoxin-interacting protein has pro-oxidant properties because it inhibits thioredoxin and enhances *nox4* expression under diabetic conditions (34).

NADPH oxidase 4 (NOX4) is a constitutively-active NADPH oxidase that generates predominantly H_2O_2, and is transcriptionally upregulated by a variety of cellular stresses, including high glucose (35,36). High glucose increased *nox4* mRNA and protein in mouse and human POBs, with cinaciguat preventing the upregulation; *nox2* expression was not altered under these conditions (Fig. 6*A–C* and Supplementary Fig. 6*A* and *B*). Cinaciguat's suppression of *nox4* mRNA was cGMP and PKG2 mediated and was mimicked by tempol, suggesting a mechanism linked to ROS (Fig. 6*D* and *E*). *Trx1* mRNA regulation was reciprocal to that of *nox4*: *trx1* was downregulated in high glucose, cinaciguat and tempol increased its expression, and cinaciguat's effect required PKG2 (Fig. 6*F* and *G*). Cinaciguat, cGMP, and tempol did not affect *nox4* or *trx1* mRNA under low glucose conditions, suggesting regulation occurred only under high oxidative stress (Supplementary Fig. 6*C* and *D*).

To evaluate whether NOX4 upregulation could account for the increased H_2O_2 production in POBs exposed to high

vs. virus encoding GCA for 48 h before measuring *prkg1* and *2* mRNAs. Graphs show mean ± SD of three to four independent experiments. By ANOVA (or *t* test in *H* and *I*): *$P < 0.05$, **$P < 0.01$, ***$P < 0.001$ for the indicated comparisons or comparison with vehicle (*C* and *K*) or GFP (*L*); and #$P < 0.05$, ##$P < 0.01$, ###$P < 0.001$ for comparison between control and diabetic osteoblasts treated with the same drug concentration (*C* and *D*) or between absence and presence of tempol (*F*).

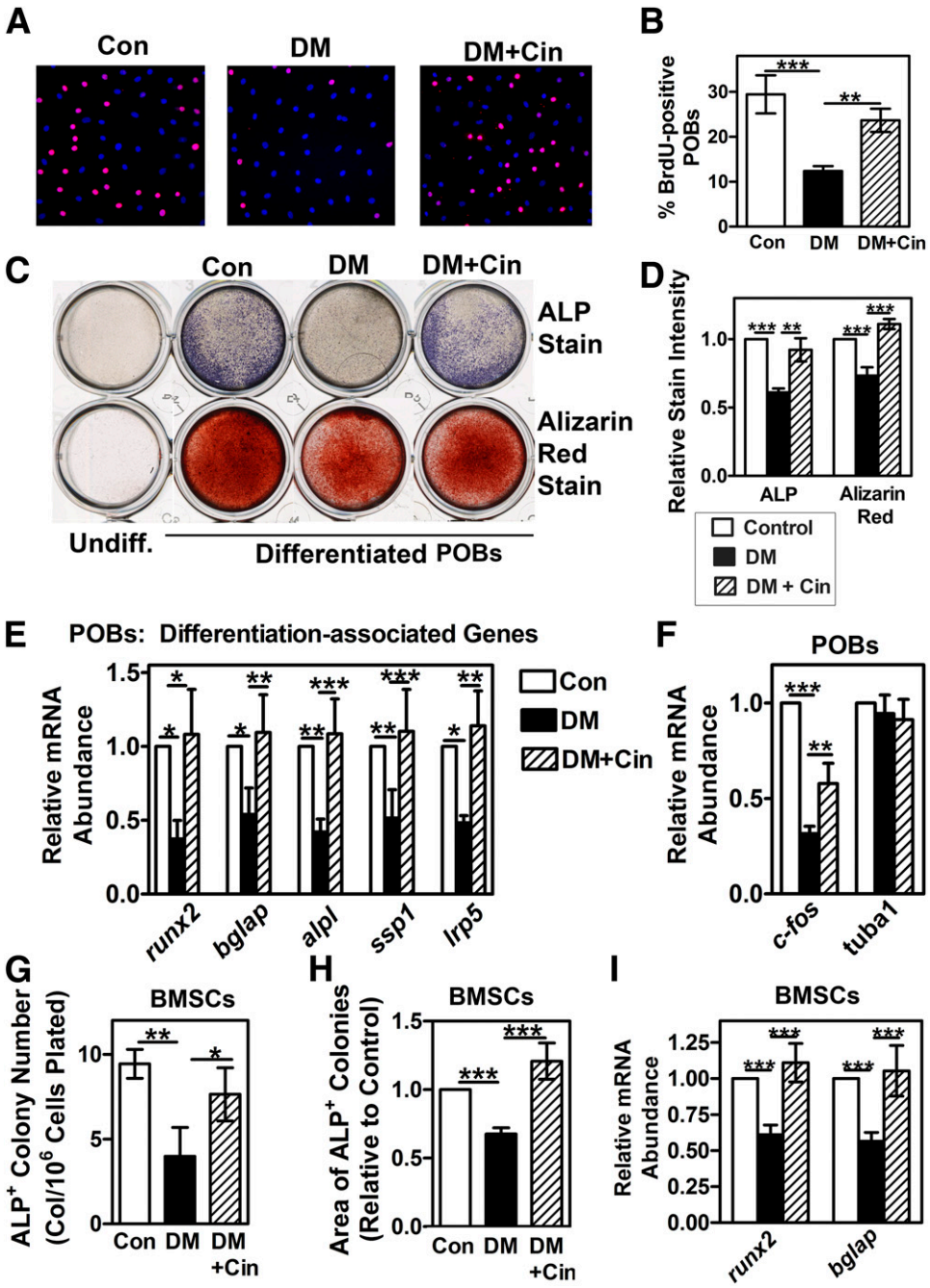

Figure 4—Restoration of diabetic preosteoblast proliferation and differentiation by cinaciguat. POBs (*A–F*) and BMSCs (*G–I*) were isolated from control mice, diabetic mice, or diabetic mice treated with cinaciguat. According to their origin, cells were cultured in 5 mmol/L glucose (Con), 25 mmol/L glucose (DM), or 25 mmol/L glucose plus 0.1 μmol/L cinaciguat (DM+Cin). Cells in panels *C–E* were grown to confluence and then transferred to osteoblastic differentiation medium maintaining the same conditions. *A* and *B*: BrdU incorporation into S-phase nuclei was determined by immunofluorescence staining (red; DNA was counterstained blue with Hoechst 33342). *C* and *D*: POBs transferred to differentiation medium for 14 or 21 days were stained for ALP activity or mineralization (Alizarin Red), respectively. *E* and *F*: Gene expression was analyzed by quantitative RT-PCR, data were normalized to 18S rRNA, and expression in control POBs was assigned a value of 1 (*bglap*, osteocalcin; *alpl*, ALP; *spp1*, osteopontin; *lrp5*, LDL receptor-related protein-5; *tuba1*, tubulin-α1). *G–I*: BMSCs were cultured in osteoblastic differentiation medium for 14 days. Cells were stained for ALP activity (*G* and *H*), and *runx2* and *bglap* mRNA expression were assessed by quantitative RT-PCR (*I*). Data are the mean ± SD of three to five independent experiments. $^*P < 0.05$, $^{**}P < 0.01$, $^{***}P < 0.001$ for the indicated comparisons by ANOVA.

glucose, we used a gene silencing approach. Short hairpin (sh)RNA–mediated knockdown of *nox4* decreased H_2O_2 production and lipid peroxidation in human POBs in high glucose to values found in control POBs in low glucose; in contrast, the *nox4* shRNA had little effect on basal H_2O_2 production and lipid peroxidation in cells in low glucose (Fig. 6*H* and *I*; Fig. 6*J* shows efficient NOX4 depletion by the shRNA). These results indicate *nox4* upregulation is

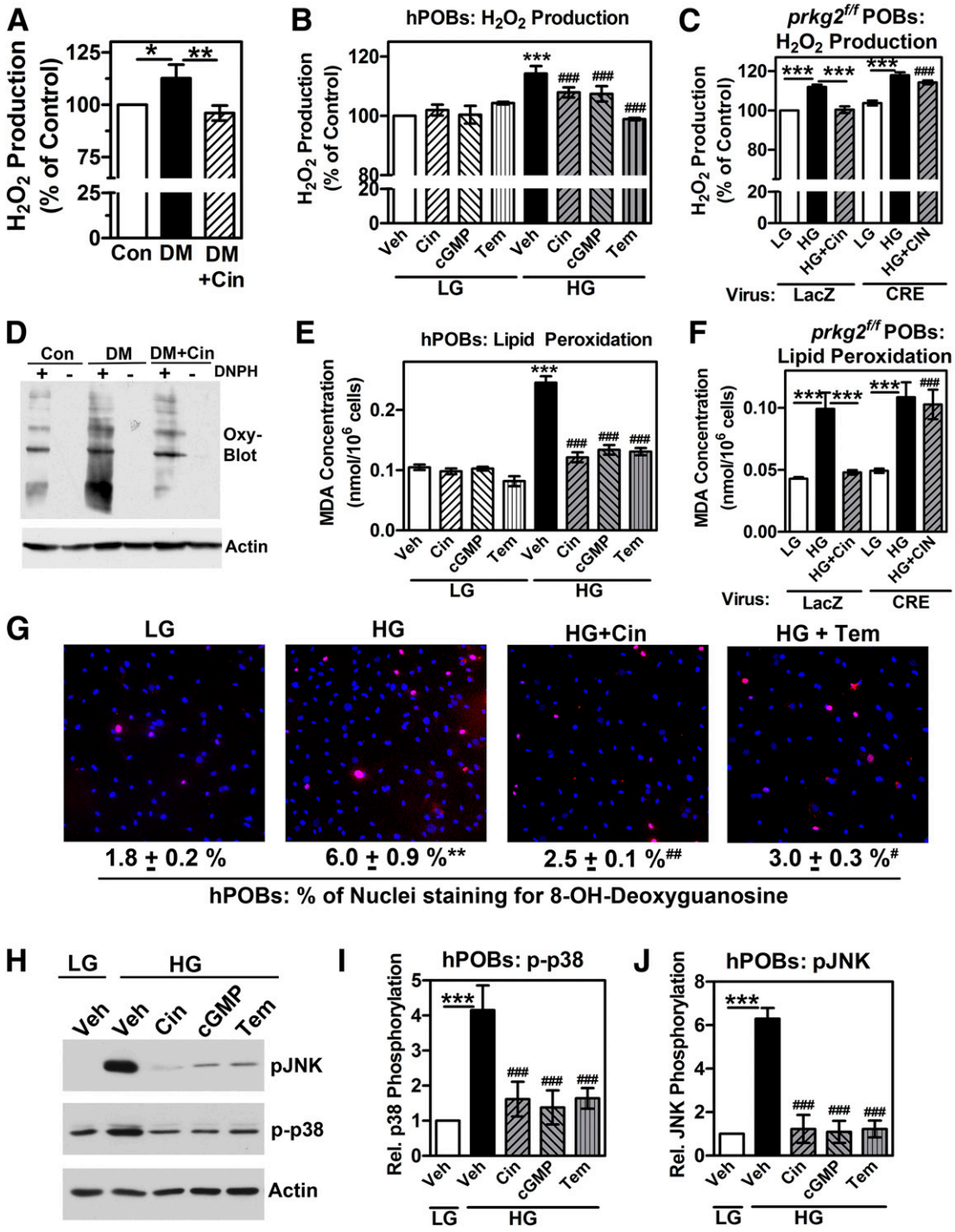

Figure 5—Reduction of oxidative stress by cinaciguat. *A* and *D*: POBs were isolated from control mice (Con), diabetic mice (DM), or diabetic mice treated with cinaciguat (DM+Cin) and were cultured as described in Fig. 4. *B*, *E*, and *G–J*: Human (h)POBs were cultured in 5 mmol/L (low) glucose (LG) or 25 mmol/L (high) glucose (HG) for 3 weeks; some cells received cinaciguat (Cin, 0.1 μmol/L), 8-CPT–cGMP (cGMP, 100 μmol/L), or tempol (Tem, 200 μmol/L) for the last 48 h, as indicated. *C* and *F*: POBs were isolated from "floxed" *prkg2*$^{f/f}$ mice. Cells were cultured in LG or HG for 3 weeks, infected with control virus (LacZ) or virus expressing CRE-recombinase (CRE), and treated with cinaciguat for 48 h. *A–C*: H_2O_2 production was measured by Amplex Red fluorescence and normalized to cellular protein content, with control cells assigned a value of 100%. *D*: Protein carbamylation was detected using OxyBlot after derivatization with 2,4-dinitrophenylhydrazine (+DNPH); nonderivatized extracts served as controls (−). *E* and *F*: Malondialdehyde (MDA) concentrations were measured to estimate lipid peroxidation products. *G*: Oxidative DNA damage was assessed by immunofluorescence using an 8-OH-deoxyguanosine–specific antibody (red; DNA counterstained blue with Hoechst 33342); the percentage of red-fluorescent nuclei is shown below ($n = 3$). $^{**}P < 0.01$ compared with LG, $\#P < 0.05$ and $\#\#P < 0.01$ compared with HG+vehicle. *H–J*: JNK and p38 activation was evaluated using phospho (p)-specific antibodies and densitometry scanning of Western blots. Graphs represent mean ± SD of three to six independent experiments. By ANOVA $^{*}P < 0.05$, $^{**}P < 0.01$, $^{***}P < 0.001$ for the indicated comparisons, and $\#\#\#P < 0.001$ for drug-treated compared with vehicle-treated cells in HG.

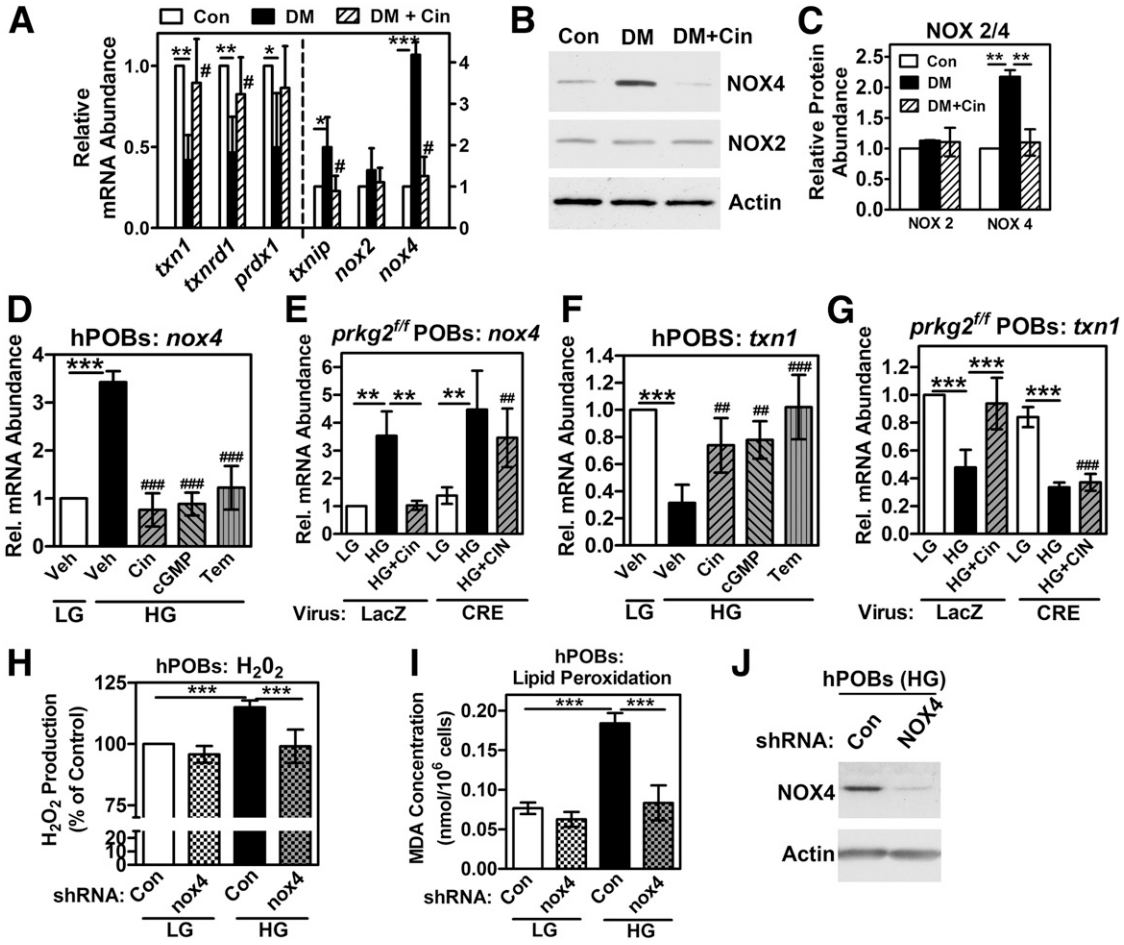

Figure 6—Regulation of thioredoxin-related genes and *nox4* by cinaciguat; NOX4 as a major ROS source in POBs exposed to high glucose. *A–C*: POBs were isolated from control mice (Con), diabetic mice (DM), or diabetic mice treated with cinaciguat (DM+Cin); cells were cultured and gene expression was analyzed as described in Fig. 4*E*. *B* and *C*: NOX2 and NOX4 protein expression was assessed by Western blotting and densitometry scanning. *D–G*: *nox4* and *trx1* mRNA abundance was measured in human (h)POBs (*D* and *F*) and in POBs isolated from "floxed" *prkg2*$^{f/f}$ mice infected with control (LacZ) or CRE virus (*E* and *G*) and cultured in 5 mmol/L (low) glucose (LG) or 25 mmol/L (high) glucose (HG); some cells were treated with Cin, cGMP, or tempol (Tem), as described in Fig. 5*B*. *H–J*: Human POBs cultured in LG or HG were infected with adenovirus encoding *nox4* shRNA or control shRNA; 48 h later, H_2O_2 production (*H*) and lipid peroxidation (*I*) were measured as in Fig. 5*B*, and NOX4 protein was assessed by Western blotting (*J*). Data represent mean ± SD of three to six independent experiments. By ANOVA $^*P < 0.05$, $^{**}P < 0.01$, $^{***}P < 0.001$ for the indicated comparisons, $\#P < 0.05$ for DM+Cin compared with DM+vehicle (panel *A*), and $\#\#P < 0.01$ and $\#\#\#P < 0.001$ for drug-treated compared with vehicle-treated cells in HG (*D–G*).

largely responsible for increased H_2O_2 production in POBs in high glucose, and cinaciguat reduces oxidative stress under hyperglycemic conditions by suppressing *nox4* and *txnip* and inducing antioxidant genes.

Cinaciguat Treatment of Diabetic Mice Improves Bone Microarchitecture and Bone Formation, While Decreasing Resorption

To induce type 1 diabetes, we administered streptozotocin to mice (7), and after 3 weeks—when the mice had been hyperglycemic for at least 1 week—we began administering a 4-week course of daily cinaciguat (Fig. 7*A* and Supplementary Table 1). In the diabetic mice, serum cGMP concentrations were decreased by >60% compared with nondiabetic animals, similar to patients with type 1 diabetes (37), and cinaciguat largely restored concentrations to normal (Fig. 7*B*). As observed in osteoblasts from diabetic mice in vitro, *prkg1* and *prkg2* mRNAs were reduced in bones of diabetic mice, whereas *nos3* mRNA was unchanged. Cinaciguat restored *prkg1* expression but had little effect on *prkg2* mRNA (Fig. 7*C*).

Micro-CT analysis of tibial bone showed decreased trabecular bone volume fraction, trabecular number, and cortical cross-sectional bone area in diabetic mice, with cinaciguat treatment improving all three parameters (Fig. 7*D–F*). Mineral apposition rate, mineralizing surface per bone surface, and bone formation rate (BFR) were dramatically decreased in the diabetic mice, as described before (9), but cinaciguat largely restored these parameters, indicating improved osteoblastic activity (Fig. 7*G–J*).

Consistent with previous reports, trabecular and cortical osteoblast numbers were reduced and osteocyte apoptosis

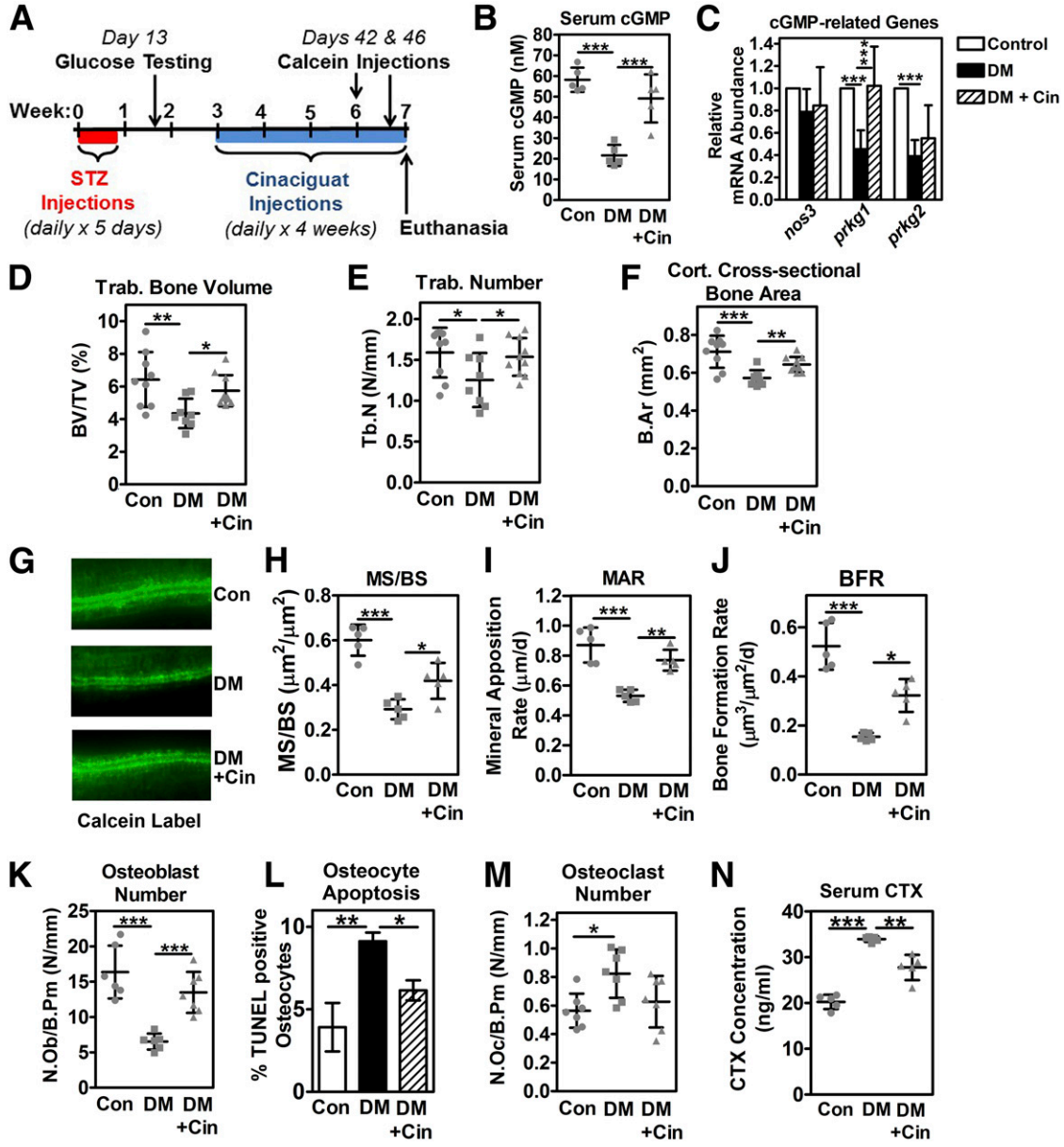

Figure 7—Cinaciguat effects in diabetic mice: increased serum cGMP, improved bone microarchitecture and bone formation, and reduced resorption. *A*: Male C57BL/6 mice (12 weeks old) were treated with vehicle (Con) or injected with streptozotocin (STZ; 40 mg/kg/day i.p.) for 5 days. Blood glucose was measured 13 days after the start of injections, and STZ-administered mice that were hyperglycemic (>270 mg/dL) received vehicle (0.1% DMSO; DM) or cinaciguat (10 μg/kg/day i.p.; DM+Cin) for 4 weeks, starting 21 days after the start of STZ injections. At 7 and 4 days before euthanasia, the mice received calcein (25 mg/kg i.p.). *B*: Serum cGMP concentrations were measured by ELISA 1 h after the last cinaciguat injection. *C*: Expression of *nos3* and *prkg1* and *2* mRNA was measured by quantitative RT-PCR in tibial bone after removal of periosteum and bone marrow and was normalized to 18S rRNA; the means of the control group were assigned a value of 1. Bone volume (BV)-to-trabecular volume (TV) fraction (*D*), trabecular number (*E*), and cortical cross-sectional bone area (*F*) were measured by micro-CT at the proximal (*D* and *E*) or midtibia (*F*). Calcein labeling was assessed at endosteal femoral surfaces (*G*) to determine mineralizing surface per bone surface (MS/BS) (*H*), mineral apposition rates (MAR) (*I*), and BFR (*J*). *K*: Osteoblasts (Ob) were counted on trabecular bone surfaces. B.Pm, bone perimeter; N., number. *L*: Osteocyte (Oc) apoptosis was assessed by TUNEL staining of femoral cortex sections. *M*: Osteoclasts were counted on trabecular bone surfaces. *N*: Serum CTX concentrations were measured by ELISA. (n = 5–7 mice/group, except n = 8–10 mice/group for panels *D*–*F*.) $^*P < 0.05$, $^{**}P < 0.01$, $^{***}P < 0.001$ for the indicated comparisons (by ANOVA).

was increased in the diabetic mice (9,13); cinaciguat almost completely reversed these changes (Fig. 7*K* and *L* and Supplementary Fig. 7*A* and *B*). Osteoclast number and serum concentrations of the osteoclast activity marker COOH-terminal telopeptide of type 1 collagen (CTX) were increased in the diabetic mice (Fig. 7*M* and *N*), as observed by some but not all investigators (9,13,38). Cinaciguat-treated diabetic animals showed reduced serum CTX concentrations and a trend toward reduced osteoclast numbers (Fig. 7*M* and *N*).

Histological examination of femur sections revealed an increase in bone marrow adiposity in the diabetic mice (Supplementary Fig. 7*C* and *D*), which is thought to be due to increased adipogenic differentiation of mesenchymal stem cells (2). Cinaciguat treatment slightly decreased the percentage of bone marrow occupied by fat cells, but this trend did not reach significance (Supplementary Fig. 7*C* and *D*). cGMP/PKG can stimulate vasculogenesis via induction of vascular endothelial growth factor-A (VEGF-A), and VEGF-A is expressed by osteoblasts (39,40). We found decreased *vegfa* mRNA and a trend toward reduced microvessel density in the bones of mice with streptozotocin-induced diabetes. Cinaciguat restored *vegfa* mRNA to levels found in control mice and caused a trend toward improved bone marrow microvascular density in diabetic mice, but the latter change did not reach statistical significance (Supplementary Fig. 8*A*–*C*).

These data indicate that cinaciguat largely reverses the negative effects of diabetes on trabecular and cortical bone by increasing osteoblast number and bone formation parameters while reducing osteoclast activity; however, the drug had only minor effects on bone marrow adiposity and microvessel density.

Cinaciguat Restores Osteoblastic and Osteoclastic Gene Expression to Control Levels and Reduces Oxidative Stress in Diabetic Bone

Concomitant with the decrease in osteoblast number and bone formation, expression of osteoblast differentiation–associated genes (*dlx1*, *runx2*, *sp7*, *bglap*, *lrp5*) was reduced in the bones of diabetic mice, but cinaciguat restored expression to levels found in control mice (Fig. 8*A*), analogous to its effect in POBs in vitro (Fig. 4*E*). The Wnt antagonist sclerostin (*sost*) is produced predominantly by osteocytes. Its expression was increased in diabetic animals, as previously reported (13), but cinaciguat reduced *sost* mRNA to control levels (Fig. 8*A*; tubulin mRNA was unchanged under all conditions). Consistent with the increase in osteoclast numbers, osteoclast-specific gene expression (*acp5*, *ctsk*) was increased in the bones of diabetic mice, with cinaciguat reducing expression to control levels (Fig. 8*B*).

Malondialdehyde concentrations, marking lipid peroxidation end products, were elevated in the serum of mice with type 1 diabetes compared with control mice (Fig. 8*C*), similar to results in patients with type 1 diabetes (37). However, cinaciguat treatment returned malondialdehyde to control levels (Fig. 8*C*). Osteocyte nuclear 8-OH-deoxyguanosine content, marking DNA oxidation, was increased in the diabetic mice, but cinaciguat restored this marker back to control levels (Fig. 8*D*). Consistent with depletion of antioxidant defense mechanisms in diabetic tissues (15), thioredoxin-related antioxidant genes were reduced in diabetic bones, while the pro-oxidant gene *txnip1* was increased (Fig. 8*E*). *nox4* mRNA was dramatically induced in diabetic bones, whereas *nox2* was unchanged (Fig. 8*F*). Cinaciguat reversed these gene expression changes in diabetic bones (Fig. 8*E* and *F*), similar to its effects in POBs (Fig. 6*A*).

Thus, cinaciguat reduced oxidative stress markers, improved bone formation, and prevented bone loss in diabetic mice, suggesting that activators of oxidized guanylate cyclase may represent a new class of bone anabolic agents for diabetic osteoporosis.

DISCUSSION

Compared with other diabetic complications, diabetic bone disease has received relatively little attention, and treatment of diabetic osteoporosis remains unsatisfactory (5). Bisphosphonates, which inhibit bone resorption, can improve bone mineral density but may worsen bone quality by repressing bone formation (1,38). Parathyroid hormone analogs, the only U.S. Food and Drug Administration–approved drugs that stimulate bone formation, have not been studied in patients with diabetes (1,41). A better understanding of the molecular mechanisms underlying diabetic bone loss is needed to design safe and effective therapies, especially in patients with suboptimal glycemic control. We now describe several findings that could lead to a novel adjunct therapy for diabetic osteoporosis (Fig. 8*G*): *1*) insulin stimulation of osteoblast proliferation and survival requires NO/cGMP/PKG2 signaling; *2*) each step of the NO/cGMP/PKG2 pathway is impaired in osteoblasts under hyperglycemic conditions; *3*) cinaciguat, via cGMP/PKG2, exerts potent antioxidant effects in diabetic osteoblasts; and *4*) cinaciguat improves bone formation and reduces bone loss in mice with type 1 diabetes by restoring impaired osteoblast proliferation, differentiation, and survival, constraining osteoclast activity, and reducing oxidative stress.

Insulin Signaling in Osteoblasts

Insulin promotes proliferation, survival, and differentiation of osteoblasts via insulin receptor activation of the Ras/Raf/mitogen-activated protein kinase kinase (MEK)/ERK and phosphatidylinositol 3-kinase (PI3K)/Akt pathways, and mice lacking the insulin receptor in osteoblasts are osteopenic (12). In mice with type 1 diabetes, insulin therapy improves bone formation and partly preserves bone volume (12,42). We found that insulin requires NO/cGMP/PKG signaling for its prosurvival and proproliferative effects in osteoblasts. Although we did not study insulin signaling in vivo, we observed decreased insulin activation of the NO/cGMP/PKG2 pathway in osteoblasts exposed to high glucose, suggesting the bone-anabolic effects of insulin are diminished under hyperglycemic conditions. Consistent with this hypothesis, high-dose continuous insulin infusion only partly prevented bone loss in mice with type 1 diabetes, in which blood glucose remained above nondiabetic levels (42).

FOXO transcription factors are important insulin targets, with insulin restraining FOXO activation and nuclear translocation via PI3K/Akt. FOXOs 1, 3, and 4 influence osteoblast proliferation, survival and resistance to oxidative stress (43). Mice with a deficiency of FOXO1 in Col1A-CRE–expressing osteoblastic cells have low bone volume with decreased osteoblast number and BFR, without change in

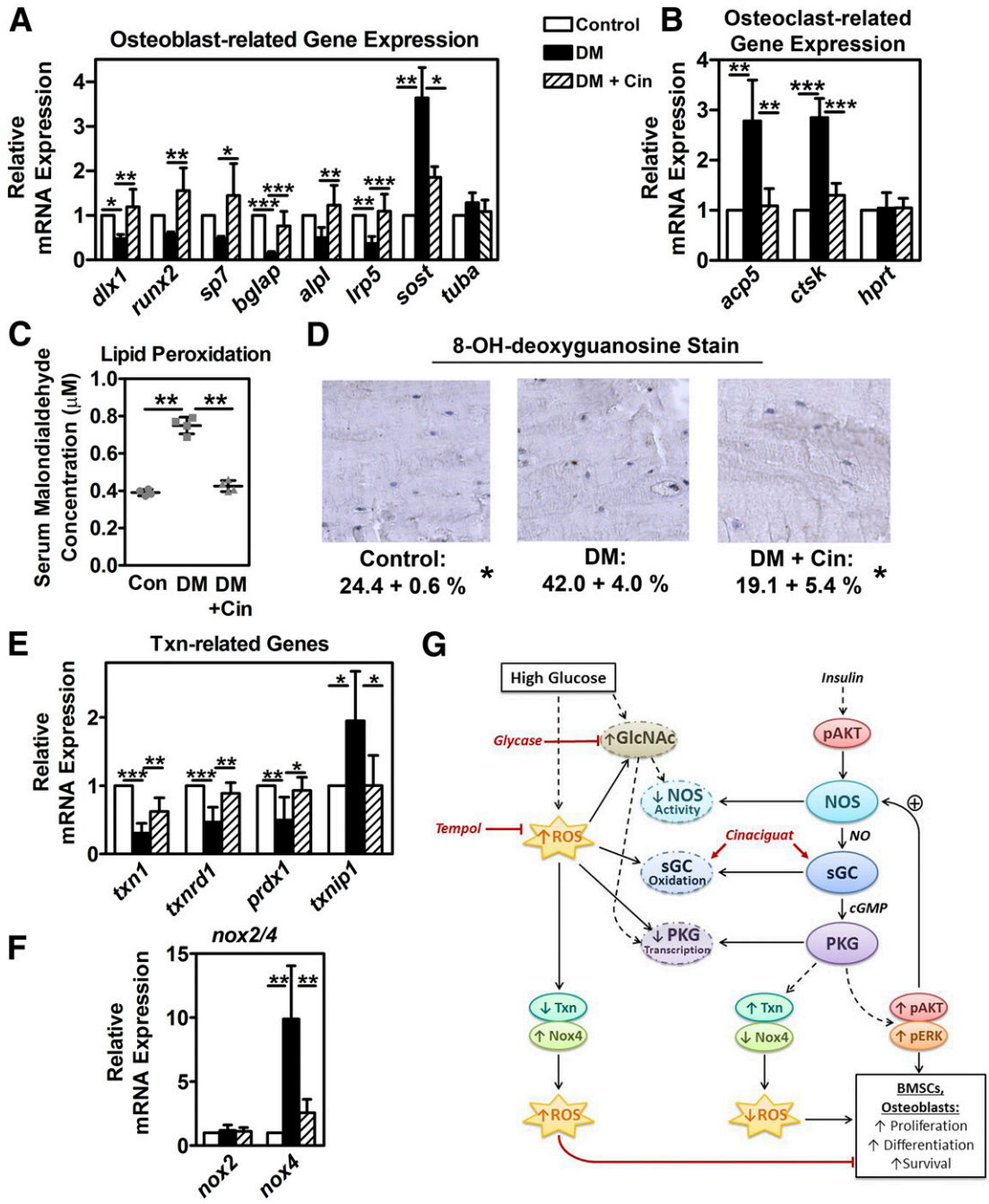

Figure 8—Cinaciguat effects in diabetic mice: regulation of osteoblast- and osteoclast-related gene expression and reduction of oxidative stress. Type 1 diabetes was induced, and diabetic mice were treated with vehicle (DM) or cinaciguat (DM+Cin) as described in Fig. 7*A*. *A* and *B*: Gene expression was measured in tibial bone and normalized to 18S rRNA as described in Fig. 7*C*. The means of the control group were assigned a value of 1 (*dlx1*, distal-less homeobox-1; *sp7*, osterix; *bglap*, osteocalcin; *alpl*, ALP; *lrp5*, LDL receptor-related protein-5; *sost*, sclerostin; *tuba1*, tubulin-α1; *acp5*, tartrate-resistant acid phosphatase; *ctsk*, cathepsin K; *hprt*, hypoxanthine phosphoribosyltransferase). *C*: Serum malondialdehyde concentrations were measured spectrophotometrically to assess lipid peroxidation. *D*: Osteocyte oxidative DNA damage was assessed by immunohistochemical staining of femoral cortex with an 8-OH-deoxyguanosine–specific antibody (black). The percentage of black cells is shown below. *E* and *F*: Gene expression was measured as in panel *A*. *A*–*F*: n = 5–7 mice/group. $^{*}P < 0.05$, $^{**}P < 0.01$, $^{***}P < 0.001$ for the indicated comparisons, except in panel *D*, $^{*}P < 0.05$ for the comparison with diabetic, vehicle-treated mice (by ANOVA). *G*: Insulin activates NO/cGMP/PKG signaling via Akt, and insulin stimulation of osteoblast proliferation and survival requires a positive feedback loop involving cGMP/PKG activation of Akt. Under hyperglycemic conditions, each step of the NO/cGMP/PKG pathway is impaired: NOS activity is reduced by *O*-GlcNAc modification, sGC activity and NO responsiveness is reduced by oxidation of the enzyme's heme group, and PKG1 and 2 transcription is downregulated by ROS- and *O*-GlcNAc-sensitive transcriptional regulators. Cinaciguat activates oxidized sGC in an NO-independent fashion and exerts antioxidant effects via cGMP activation of PKG2, by downregulating NOX4 and upregulating thioredoxin family antioxidant proteins. Reduction of ROS improves proliferation and survival of osteoblasts and their precursors.

osteoblast apoptosis (44). In contrast, deletion of FOXOs 1/3/4 in osteoblast progenitors via Osx1-CRE increases osteoblast number, BFR, and cortical bone volume, and attenuates diabetes-induced trabecular bone loss, without correcting low BFR or cortical bone loss in mice with type 1 diabetes (43). Because we found cGMP-dependent Akt activation in osteoblasts, some of the bone-protective effects of cinaciguat in diabetic mice could be explained by inhibition of FOXO transcription. However, the roles of FOXOs in bone are complex, and more work is required to define the role of each FOXO family member.

Defective NO/cGMP Signaling in Diabetes

Endothelial NO generation and serum nitrite/nitrate and cGMP concentrations are reduced in patients with diabetes, similar to our finding of reduced serum cGMP in diabetic mice (20,37); however, few studies have addressed cGMP/PKG signaling downstream of NO under diabetic conditions (19). Consistent with our results in osteoblasts, *O*-GlcNAc modification of NOS3 is increased approximately twofold in endothelial cells exposed to high glucose or isolated from diabetic mice compared with control cells (17,45). *O*-GlcNAc modification of NOS3 occurs predominantly on Ser^{1177} and blocks phosphorylation and activation of NOS3 by Akt, but NOS association with HSP90 and caveolin-1 was not studied previously under diabetic conditions (17,30). We saw no evidence of uncoupled NOS activity in diabetic osteoblasts, in contrast to what occurs in diabetic endothelium (19).

We found oxidative stress reduced sGC activation and downregulated PKG1 and 2 transcription under hyperglycemic conditions in vitro and in vivo. The reduced NO-responsiveness of sGC in POBs exposed to high glucose was due to oxidation of the enzyme's heme iron rather than to reduced enzyme levels, because *1*) cinaciguat, which can activate oxidized (Fe^{3+}) and reduced (Fe^{2+}) sGC, stimulated cGMP synthesis similarly in POBs in high and low glucose, whereas riociguat and NO, which activate only reduced (Fe^{2+}) sGC, were much more effective in low than in high glucose, despite similar levels of the heme-containing β-subunit of sGC; and *2*) the ROS-quenching agent tempol increased cGMP synthesis more than fivefold in response to riociguat or NO in POBs in high glucose, whereas the antioxidant had no effect in low glucose (32,33). The NO/cGMP/PKG signaling defects observed in high glucose were reversible, albeit slowly: *1*) basal and insulin-induced NOS activity were improved by removing *O*-GlcNAc modifications; *2*) NO-induced cGMP synthesis was improved by tempol, and cGMP synthesis was restored by cinaciguat; and *3*) *prkg1/2* transcriptional downregulation was reversed by tempol or glycase. After osteoblasts were transferred from high to low glucose medium, *prkg1/2* transcription gradually increased, compatible with loss of *O*-GlcNAc modifications due to slow protein turnover. SP-1 is a ROS-sensitive transcriptional regulator modified by *O*-GlcNAc and required for *prkg1* promoter activity (18). Other candidate transcription factors include Nrf-2, and we are presently characterizing oxidative stress–responsive transcriptional regulators and high glucose–induced changes in the osteoblast transcriptome. Thus, hyperglycemia alters NO/cGMP/PKG signaling at every step, leading to long-term cellular dysfunction even after correction of hyperglycemia (hyperglycemic memory).

Oxidative Stress in Diabetes

Biomarkers of oxidative stress are elevated in patients with type 1 and 2 diabetes, and increased oxidative stress contributes to the development of diabetic cardiovascular and kidney disease (15,46). Oxidative stress also appears to contribute to diabetic bone loss, because *1*) transgenic overexpression of thioredoxin attenuates osteoporosis in mice with streptozotocin-induced diabetes (16); *2*) antioxidant flavonoids improve bone volume in rats with type 1 diabetes (47); and *3*) oxidative stress inhibits osteoblast differentiation and induces osteoblast death in vitro (48).

Increased ROS production in diabetic tissues has been attributed to increased NADPH oxidase activity, NOS uncoupling, and enhanced mitochondrial superoxide (O_2^-) production (15,19,34,49,50). We identified *nox4* upregulation as the major source of increased H_2O_2 and oxidative stress in diabetic osteoblasts and bones: shRNA-mediated *nox4* depletion reduced H_2O_2 production and lipid peroxidation in osteoblasts in high glucose to values found in low glucose, and cinaciguat reduced *nox4* mRNA expression and DNA oxidation in femurs of diabetic mice to values in control mice. Increased *nox4* expression has been observed in diabetic heart and kidney, and global *nox4* deletion alleviates diabetes-induced kidney injury (51). How NOX4 contributes to diabetic bone loss will require generating osteoblast-specific *nox4* knockout mice, because global $nox4^{-/-}$ mice have a high bone mass due to reduced osteoclast numbers and activity (52).

Mitochondrial O_2^- and H_2O_2 production contribute to age-related bone loss, based on mice lacking mitochondrial superoxide dismutase or expressing mitochondrial-targeted catalase in osteoblastic cells, respectively (53,54). We found increased mitochondrial O_2^- production in POBs exposed to high glucose. NOX4 localizes to both plasma membranes and mitochondria and may contribute to mitochondrial O_2^- and H_2O_2 production (36,51).

Antioxidant Effects of cGMP/PKG2

We uncovered novel antioxidant functions of cGMP in osteoblasts cultured in high glucose: cinaciguat and 8-CPT–cGMP increased the antioxidant genes *txn1*, *txnrd1*, and *prdx1*, while simultaneously downregulating the pro-oxidant genes *nox4* and *txnip*. Cinaciguat induced the same changes in bone of diabetic mice and reduced markers of DNA oxidation under hyperglycemic conditions in vivo. Cinaciguat, 8-CPT–cGMP, and tempol did not change *nox4* or *txn1* mRNA under normoglycemic conditions, suggesting *nox4* and *txn1* are regulated by ROS-responsive transcription factors in hyperglycemic cells. We found that the antioxidant effects of cGMP in osteoblasts were mediated by

PKG2, whereas antioxidant effects of cGMP in endothelial cells are attributed to PKG1 posttranscriptionally upregulating catalase and glutathione peroxidase (55).

Anabolic Effects of Cinaciguat in Diabetic Bone

We identified reduced NO/cGMP/PKG signaling as a major mechanism of diabetic bone loss and showed that restoring cGMP synthesis with cinaciguat in type 1 diabetic mice reduced oxidative stress, improved bone formation, and attenuated trabecular and cortical bone loss. We showed previously that cinaciguat protects mice from ovariectomy-induced trabecular bone loss, but the drug had no significant effect on bone microarchitecture in control mice (26). Cinaciguat reduced osteocyte apoptosis in ovariectomized and in diabetic mice. This antiapoptotic effect likely contributes to bone protection in both disease models because osteocyte apoptosis has been causally linked to trabecular and cortical bone loss (54,56). We found that cinaciguat increased expression of *runx2* and *bglap* mRNA in vivo and in POBs and BMSCs in vitro, suggesting a stimulatory effect on osteoblastic differentiation. In contrast, Jafari et al. (57) found that the nonspecific protein kinase inhibitor H-8 promoted osteoblast differentiation of telomerase-overexpressing human BMSCs and suggested the effect of H-8 was via PKG1 inhibition because it was partly mimicked by small interfering RNA knockdown of PKG1. The differences in our results and those obtained by Jafari et al. (57) could be due to differences in cell type and differentiation protocol but could also relate to off-target effects of a nonspecific protein kinase inhibitor.

Cinaciguat is a prototype of recently developed NO- and heme-independent sGC activators, and, other than hypotension at high doses, was well tolerated in clinical trials of cardiovascular diseases (32). The cinaciguat dose we used does not affect systolic blood pressure (26). We conclude that hyperglycemia-induced disruption of NO/cGMP/PKG signaling contributes to oxidative stress and bone loss in mice with type 1 diabetes and that NO/cGMP/PKG pathway activators present a novel paradigm for enhancing bone formation under conditions of hyperglycemia and oxidative stress.

Acknowledgments. The authors are grateful to Esther Cory (University of California, San Diego), Jennifer Santini (University of California, San Diego), and Dezhi Wang (The University of Alabama) for their expert assistance and thank Dr. Hemal Patel (University of California, San Diego) for providing the *nox4* shRNA adenoviral construct.

Funding. W.D. received support from the P. Robert Majumder Charitable Foundation. This work was supported by National Institute of Arthritis and Musculoskeletal Skin Diseases (NIAMS) grant P01-AG-007996 (to R.L.S.), National Cancer Institute (NCI) grant P30-CA-023100 (to University of California, San Diego Gene Targeting and Transgenic Mouse Core), National Institute of Neurological Disorders and Stroke grant P30-NS-047101 (to University of California, San Diego Neuroscience Microscopy Shared Facility), and NIAMS grant P30-AR-04603 (to University of Alabama, Birmingham, Center for Metabolic Bone Disease), and NIAMS grants R01-AR068601 and R21-AR065658 (to R.B.P.).

Duality of Interest. No potential conflicts of interest relevant to this article were reported.

Author Contributions. H.K., G.S., G.R., F.C., B.T.S., and D.E.C. contributed to the conduct of study. H.K., W.D., R.L.S., and R.B.P. contributed to data interpretation. H.K. and D.E.C. contributed to data collection. H.K. and R.B.P. contributed to study design and data analysis and drafted the manuscript. H.K. and R.B.P. are the guarantors of this work and, as such, had full access to all the data in the study and take responsibility for the integrity of the data and the accuracy of the data analysis.

References

1. Napoli N, Chandran M, Pierroz DD, Abrahamsen B, Schwartz AV, Ferrari SL; IOF Bone and Diabetes Working Group. Mechanisms of diabetes mellitus-induced bone fragility. Nat Rev Endocrinol 2017;13:208–219
2. McCabe L, Zhang J, Raehtz S. Understanding the skeletal pathology of type 1 and 2 diabetes mellitus. Crit Rev Eukaryot Gene Expr 2011;21:187–206
3. Weber DR, Schwartz G. Epidemiology of skeletal health in type 1 diabetes. Curr Osteoporos Rep 2016;14:327–336
4. Weber DR, Haynes K, Leonard MB, Willi SM, Denburg MR. Type 1 diabetes is associated with an increased risk of fracture across the life span: a population-based cohort study using The Health Improvement Network (THIN). Diabetes Care 2015;38:1913–1920
5. Sellmeyer DE, Civitelli R, Hofbauer LC, Khosla S, Lecka-Czernik B, Schwartz AV. Skeletal metabolism, fracture risk, and fracture outcomes in type 1 and type 2 diabetes. Diabetes 2016;65:1757–1766
6. Hygum K, Starup-Linde J, Harsløf T, Vestergaard P, Langdahl BL. Mechanisms in endocrinology: diabetes mellitus, a state of low bone turnover – a systematic review and meta-analysis. Eur J Endocrinol 2017;176:R137–R157
7. Botolin S, McCabe LR. Bone loss and increased bone adiposity in spontaneous and pharmacologically induced diabetic mice. Endocrinology 2007;148:198–205
8. Thrailkill KM, Liu L, Wahl EC, et al. Bone formation is impaired in a model of type 1 diabetes. Diabetes 2005;54:2875–2881
9. Hamada Y, Kitazawa S, Kitazawa R, Fujii H, Kasuga M, Fukagawa M. Histomorphometric analysis of diabetic osteopenia in streptozotocin-induced diabetic mice: a possible role of oxidative stress. Bone 2007;40:1408–1414
10. Maddaloni E, D'Eon S, Hastings S, et al. Bone health in subjects with type 1 diabetes for more than 50 years. Acta Diabetol 2017;54:479–488
11. Fowlkes JL, Bunn RC, Thrailkill KM. Contributions of the insulin/insulin-like growth factor-1 axis to diabetic osteopathy. J Diabetes Metab 2011;1: S1–003
12. Fulzele K, Riddle RC, DiGirolamo DJ, et al. Insulin receptor signaling in osteoblasts regulates postnatal bone acquisition and body composition. Cell 2010; 142:309–319
13. Kalaitzoglou E, Popescu I, Bunn RC, Fowlkes JL, Thrailkill KM. Effects of type 1 diabetes on osteoblasts, osteocytes, and osteoclasts. Curr Osteoporos Rep 2016; 14:310–319
14. Li YM, Schilling T, Benisch P, et al. Effects of high glucose on mesenchymal stem cell proliferation and differentiation. Biochem Biophys Res Commun 2007; 363:209–215
15. Giacco F, Brownlee M. Oxidative stress and diabetic complications. Circ Res 2010;107:1058–1070
16. Hamada Y, Fujii H, Kitazawa R, Yodoi J, Kitazawa S, Fukagawa M. Thioredoxin-1 overexpression in transgenic mice attenuates streptozotocin-induced diabetic osteopenia: a novel role of oxidative stress and therapeutic implications. Bone 2009;44:936–941
17. Du XL, Edelstein D, Dimmeler S, Ju Q, Sui C, Brownlee M. Hyperglycemia inhibits endothelial nitric oxide synthase activity by posttranslational modification at the Akt site. J Clin Invest 2001;108:1341–1348
18. Clark RJ, McDonough PM, Swanson E, et al. Diabetes and the accompanying hyperglycemia impairs cardiomyocyte calcium cycling through increased nuclear O-GlcNAcylation. J Biol Chem 2003;278:44230–44237
19. Hink U, Li H, Mollnau H, et al. Mechanisms underlying endothelial dysfunction in diabetes mellitus. Circ Res 2001;88:E14–E22

20. Udvardy M, Kaplar M, Rejto L, et al. Increased in vivo platelet activation and reduced intravascular endothelium-derived relaxing factor and nitrate/nitrite production in patients with insulin-dependent diabetes mellitus. Platelets 1998; 9:257–260
21. Armour KE, Armour KJ, Gallagher ME, et al. Defective bone formation and anabolic response to exogenous estrogen in mice with targeted disruption of endothelial nitric oxide synthase. Endocrinology 2001;142:760–766
22. Kalyanaraman H, Ramdani G, Joshua J, et al. A novel, direct NO donor regulates osteoblast and osteoclast functions and increases bone mass in ovariectomized mice. J Bone Miner Res 2017;32:46–59
23. Rangaswami H, Schwappacher R, Tran T, et al. Protein kinase G and focal adhesion kinase converge on Src/Akt/β-catenin signaling module in osteoblast mechanotransduction. J Biol Chem 2012;287:21509–21519
24. Rangaswami H, Schwappacher R, Marathe N, et al. Cyclic GMP and protein kinase G control a Src-containing mechanosome in osteoblasts. Sci Signal 2010;3: ra91
25. Marathe N, Rangaswami H, Zhuang S, Boss GR, Pilz RB. Pro-survival effects of 17β-estradiol on osteocytes are mediated by nitric oxide/cGMP via differential actions of cGMP-dependent protein kinases I and II. J Biol Chem 2012;287:978–988
26. Joshua J, Schwaerzer GK, Kalyanaraman H, et al. Soluble guanylate cyclase as a novel treatment target for osteoporosis. Endocrinology 2014;155:4720–4730
27. Dempster DW, Compston JE, Drezner MK, et al. Standardized nomenclature, symbols, and units for bone histomorphometry: a 2012 update of the report of the ASBMR Histomorphometry Nomenclature Committee. J Bone Miner Res 2013;28:2–17
28. Bouxsein ML, Boyd SK, Christiansen BA, Guldberg RE, Jepsen KJ, Müller R. Guidelines for assessment of bone microstructure in rodents using micro-computed tomography. J Bone Miner Res 2010;25:1468–1486
29. Zeng G, Nystrom FH, Ravichandran LV, et al. Roles for insulin receptor, PI3-kinase, and Akt in insulin-signaling pathways related to production of nitric oxide in human vascular endothelial cells. Circulation 2000;101:1539–1545
30. Förstermann U, Sessa WC. Nitric oxide synthases: regulation and function. Eur Heart J 2012;33:829–837, 837a–837d
31. Musicki B, Kramer MF, Becker RE, Burnett AL. Inactivation of phosphorylated endothelial nitric oxide synthase (Ser-1177) by O-GlcNAc in diabetes-associated erectile dysfunction. Proc Natl Acad Sci U S A 2005;102:11870–11875
32. Stasch JP, Pacher P, Evgenov OV. Soluble guanylate cyclase as an emerging therapeutic target in cardiopulmonary disease. Circulation 2011;123:2263–2273
33. Stasch JP, Schmidt PM, Nedvetsky PI, et al. Targeting the heme-oxidized nitric oxide receptor for selective vasodilatation of diseased blood vessels. J Clin Invest 2006;116:2552–2561
34. Shah A, Xia L, Goldberg H, Lee KW, Quaggin SE, Fantus IG. Thioredoxin-interacting protein mediates high glucose-induced reactive oxygen species generation by mitochondria and the NADPH oxidase, Nox4, in mesangial cells. J Biol Chem 2013;288:6835–6848
35. Xi G, Shen X, Wai C, Vilas CK, Clemmons DR. Hyperglycemia stimulates p62/PKCζ interaction, which mediates NF-κB activation, increased Nox4 expression, and inflammatory cytokine activation in vascular smooth muscle. FASEB J 2015;29: 4772–4782
36. Block K, Gorin Y, Abboud HE. Subcellular localization of Nox4 and regulation in diabetes. Proc Natl Acad Sci U S A 2009;106:14385–14390
37. Farkas K, Jermendy G, Herold M, Ruzicska E, Sasvári M, Somogyi A. Impairment of the NO/cGMP pathway in the fasting and postprandial state in type 1 diabetes mellitus. Exp Clin Endocrinol Diabetes 2004;112:258–263
38. Coe LM, Tekalur SA, Shu Y, Baumann MJ, McCabe LR. Bisphosphonate treatment of type I diabetic mice prevents early bone loss but accentuates suppression of bone formation. J Cell Physiol 2015;230:1944–1953
39. Sahara M, Sata M, Morita T, Nakajima T, Hirata Y, Nagai R. A phosphodiesterase-5 inhibitor vardenafil enhances angiogenesis through a protein kinase G-dependent hypoxia-inducible factor-1/vascular endothelial growth factor pathway. Arterioscler Thromb Vasc Biol 2010;30:1315–1324
40. Song Q, Ni J, Jiang H, Shi Z. Sildenafil improves blood perfusion in steroid-induced avascular necrosis of femoral head in rabbits via a protein kinase G-dependent mechanism. Acta Orthop Traumatol Turc 2017;51:398–403
41. Motyl KJ, McCauley LK, McCabe LR. Amelioration of type I diabetes-induced osteoporosis by parathyroid hormone is associated with improved osteoblast survival. J Cell Physiol 2012;227:1326–1334
42. Nyman JS, Kalaitzoglou E, Clay Bunn R, Uppuganti S, Thrailkill KM, Fowlkes JL. Preserving and restoring bone with continuous insulin infusion therapy in a mouse model of type 1 diabetes. Bone Rep 2017;7:1–8
43. Iyer S, Han L, Ambrogini E, et al. Deletion of FoxO1, 3, and 4 in osteoblast progenitors attenuates the loss of cancellous bone mass in a mouse model of type 1 diabetes. J Bone Miner Res 2017;32:60–69
44. Rached MT, Kode A, Xu L, et al. FoxO1 is a positive regulator of bone formation by favoring protein synthesis and resistance to oxidative stress in osteoblasts. Cell Metab 2010;11:147–160
45. Makino A, Dai A, Han Y, et al. O-GlcNAcase overexpression reverses coronary endothelial cell dysfunction in type 1 diabetic mice. Am J Physiol Cell Physiol 2015; 309:C593–C599
46. Martín-Gallán P, Carrascosa A, Gussinyé M, Domínguez C. Oxidative stress in childhood type 1 diabetes: results from a study covering the first 20 years of evolution. Free Radic Res 2007;41:919–928
47. Liang W, Luo Z, Ge S, et al. Oral administration of quercetin inhibits bone loss in rat model of diabetic osteopenia. Eur J Pharmacol 2011;670:317–324
48. Mody N, Parhami F, Sarafian TA, Demer LL. Oxidative stress modulates osteoblastic differentiation of vascular and bone cells. Free Radic Biol Med 2001; 31:509–519
49. Gao L, Mann GE. Vascular NAD(P)H oxidase activation in diabetes: a double-edged sword in redox signalling. Cardiovasc Res 2009;82:9–20
50. Nishikawa T, Edelstein D, Du XL, et al. Normalizing mitochondrial superoxide production blocks three pathways of hyperglycaemic damage. Nature 2000;404: 787–790
51. Thallas-Bonke V, Jha JC, Gray SP, et al. Nox-4 deletion reduces oxidative stress and injury by PKC-α-associated mechanisms in diabetic nephropathy. Physiol Rep 2014;2:e12192
52. Goettsch C, Babelova A, Trummer O, et al. NADPH oxidase 4 limits bone mass by promoting osteoclastogenesis. J Clin Invest 2013;123:4731–4738
53. Ucer S, Iyer S, Kim HN, et al. The effects of aging and sex steroid deficiency on the murine skeleton are independent and mechanistically distinct. J Bone Miner Res 2017;32:560–574
54. Kobayashi K, Nojiri H, Saita Y, et al. Mitochondrial superoxide in osteocytes perturbs canalicular networks in the setting of age-related osteoporosis. Sci Rep 2015;5:9148
55. Stephens RS, Servinsky LE, Rentsendorj O, Kolb TM, Pfeifer A, Pearse DB. Protein kinase G increases antioxidant function in lung microvascular endothelial cells by inhibiting the c-Abl tyrosine kinase. Am J Physiol Cell Physiol 2014;306:C559–C569
56. Tatsumi S, Ishii K, Amizuka N, et al. Targeted ablation of osteocytes induces osteoporosis with defective mechanotransduction. Cell Metab 2007;5:464–475
57. Jafari A, Siersbaek MS, Chen L, et al. Pharmacological inhibition of protein kinase G1 enhances bone formation by human skeletal stem cells through activation of RhoA-Akt signaling. Stem Cells 2015;33:2219–2231